

## DETECTION OF A 63° COLD STELLAR STREAM IN THE SLOAN DIGITAL SKY SURVEY

C. J. GRILLMAIR

*Spitzer* Science Center, 1200 East California Boulevard, Pasadena, CA 91125; carl@ipac.caltech.edu

AND

O. DIONATOS<sup>1</sup>

INAF–Osservatorio Astronomico di Roma, Via di Frascati 33, 00040, Monteporzio Catone, Italy; dionatos@mporzio.astro.it

*Received 2006 March 17; accepted 2006 April 14; published 2006 May 2*

## ABSTRACT

We report on the detection in Sloan Digital Sky Survey data of a 63°-long tidal stream of stars, extending from Ursa Major to Cancer. The stream has no obvious association with the orbit of any known cluster or galaxy. The contrast of the detected stream is greatest when using a star count filter that is matched to the color-magnitude distribution of stars in M13, which suggests that the stars making up the stream are old and metal-poor. The visible portion of the stream is very narrow and about 8.5 kpc above the Galactic disk, suggesting that the progenitor is or was a globular cluster. While the surface density of the stream varies considerably along its length, its path on the sky is very smooth and uniform, showing no evidence of perturbations by large mass concentrations in the nearby halo. While definitive constraints cannot be established without radial velocity information, the stream's projected path and estimates of its distance suggest that we are observing the stream near the perigalacticon of its orbit.

*Subject headings:* Galaxy: halo — Galaxy: structure — globular clusters: general

## 1. INTRODUCTION

Despite its still limited extent, the Sloan Digital Sky Survey (SDSS) continues to be a remarkable resource for studies of Galactic structure. In addition to the large-scale features attributed to past galaxy accretion events (Yanny et al. 2003; Majewski et al. 2003; Rocha-Pinto et al. 2004), SDSS data were used to detect the remarkably strong tidal tails of Palomar 5 (Odenkirchen et al. 2001; Rockosi et al. 2002; Odenkirchen et al. 2003). Tidal tails of globular clusters are particularly interesting from a Galactic structure standpoint as they are expected to be very numerous and to sample the Galactic potential much more uniformly than satellite galaxies. Moreover, such tidal tails are dynamically very cold (Combes et al. 1999), making them useful for constraining not only the global Galactic potential but also its lumpiness (Murali & Dubinski 1999).

Substantial tidal streams have now been found associated with at least two of the eight globular clusters in the SDSS area: Pal 5 (Odenkirchen et al. 2003; Grillmair & Dionatos 2006) and NGC 5466 (Belokurov et al. 2006; Grillmair & Johnson 2006). In this Letter we examine a much larger region of the SDSS to search for more extended structures. We briefly describe our analysis in § 2. We discuss the detection of a new stellar stream in § 3, make some initial distance estimates in § 3.1, attempt to identify a progenitor in § 3.2, and put initial constraints on the orbit in § 3.3. We make concluding remarks in § 4.

## 2. DATA ANALYSIS

Data comprising  $u'$ ,  $g'$ ,  $r'$ ,  $i'$ , and  $z'$  photometry for  $5.3 \times 10^7$  stars in the region  $124^\circ < \alpha < 251^\circ$  and  $-1^\circ < \delta < 65^\circ$  were extracted from the SDSS database using the SDSS CasJobs query system. The data were analyzed using the matched filter technique employed by Grillmair & Johnson (2006) and Grillmair & Dionatos (2006), and described in detail by Rockosi

et al. (2002). This technique is made necessary by the fact that, over the magnitude range and over the region of sky we are considering, the foreground disk stars outnumber the more distant stars in the Galactic halo by 3 orders of magnitude. Applied to the color-magnitude domain, the matched filter is a means by which we can optimally differentiate between two populations, provided we know the color-magnitude distribution of each.

In practice, we use the SDSS photometry to create a color-magnitude density or Hess diagram for both the stars of interest (e.g., those in a globular cluster) and the foreground population. Dividing the former by the latter, we generate an array of relative weights that constitute an optimal color-magnitude filter. Using this filter, every star in the survey can be assigned a weight or probability of being a member of our chosen globular cluster based on its measured magnitude and color. Having used observed data to generate it, the filter implicitly includes the effects of photometric uncertainties, and even though a particular star may lie  $3\sigma$  away from the main sequence of a globular cluster of interest, its relative weight (and thus probability of being a cluster star) may still be high if the number of foreground stars in this region of the Hess diagram is relatively low (e.g., near the horizontal branch or blueward of the main-sequence turnoff).

As we were initially interested in searching for tidal streams associated with globular clusters, we constructed Hess diagrams for each of the eight globular clusters in the SDSS Data Release 4 (DR4) area (NGC 2419, Pal 3, NGC 5272, NGC 5466, Pal 5, NGC 6205, NGC 7078, and NGC 7089). A single Hess diagram for field stars was generated using  $1.2 \times 10^7$  stars spread over  $\sim 2200 \text{ deg}^2$  of DR4. We then applied each of the eight resulting optimal filters in turn to the entire survey area. The resulting weighted star counts were summed by location on the sky to produce eight different, two-dimensional weight images or probability maps.

We used all stars with  $15 < g' < 22.5$ . We dereddened the SDSS photometry as a function of position on the sky using the DIRBE/IRAS dust maps of Schlegel et al. (1998). We op-

<sup>1</sup> Department of Physics, University of Athens, Panepistimiopolis, 15771 Athens, Greece.

timally filtered the  $g' - u'$ ,  $g' - r'$ ,  $g' - i'$ , and  $g' - z'$  star counts independently and then co-added the resulting weight images. In Figure 1 we show the final, combined, filtered star count distribution, using a filter matched to the color-magnitude distribution of stars in NGC 6205 (M13). The image has been smoothed with a Gaussian kernel with  $\sigma = 0.2$ . A low-order, polynomial surface has been subtracted from the image to approximately remove large-scale gradients due to the Galactic disk and bulge.

### 3. DISCUSSION

Quite obvious in Figure 1 is a long, remarkably smooth, curving stream of stars, extending over  $140^\circ < \alpha < 220^\circ$ . On the sky, the stream runs in an almost straight line through the whole of Ursa Major and Leo Minor, ending in Cancer and spanning a total of  $63^\circ$ . The stream is most evident when we use a filter that is matched to the color-magnitude distribution and luminosity function of stars in M13, although shifted faintward by 0.2 mag. Optimal filters based on the other seven globular clusters in DR4 did not yield the level of contrast that we see in Figure 1. The stream is easily visible in each individual color pair, including  $g' - u'$ . There may be a second, more diffuse feature with  $174 < \alpha < 200$  about  $3^\circ$  to the north of the stream, but we defer analysis of this feature to a future paper.

The stream is not a product of our dereddening procedure; careful examination of the reddening map of Schlegel et al. (1998) shows no correlation between this feature and the applied reddening corrections. The maximum values of  $E(B - V)$  are  $\approx 0.03$ , with typical values in the range 0.01–0.02 over the length of the stream. Rerunning the matched filter analysis without reddening corrections yielded little more than a slight reduction in the apparent strength of the stream.

We also ran our optimum filter against the SDSS DR4 galaxy catalog to investigate whether the stream could be due to confusion with faint galaxies. (Such a structure in the distribution of galaxies would be no less interesting than a stellar stream of these dimensions!) However, we found no feature in the filtered galaxy counts that could mimic the stream apparent in Figure 1.

At its southwestern end, the stream is truncated by the limits of the available data. We attempted to trace the stream in the portion of DR4 with  $0^\circ < \delta < 10^\circ$  but could find no convincing continuation. Plausible orbits for the stream (see below) predict a fairly narrow range of possible paths across this region and generally a rather sharp increase in Sun-stream distance. We attempted to recover the stream by shifting our filter from  $-1.0$  to  $+3.0$  mag, but to no avail. A continuation of the stream may well be there, but the power of the matched filter is significantly reduced as the bulk of the main sequence drops below the survey data's 50% completeness threshold. Combined with the rapid rise in the number of contaminating Galactic disk stars in this region, there appears to be little chance of recovering the stream until much deeper surveys become available.

On the northeastern end, the stream becomes indiscernible beyond R.A. =  $220^\circ$ . We attempted to enhance the northeastern end of the stream by shifting the filter to both brighter and fainter magnitudes, but again to no avail. Experiments in which we inserted artificial stellar streams with surface densities similar to those observed in Figure 1 revealed that they too largely vanished beyond R.A. =  $220^\circ$ . Hence, while it is conceivable that we are seeing the physical end of the stream, it is equally possible that our failure to trace the stream any further reflects

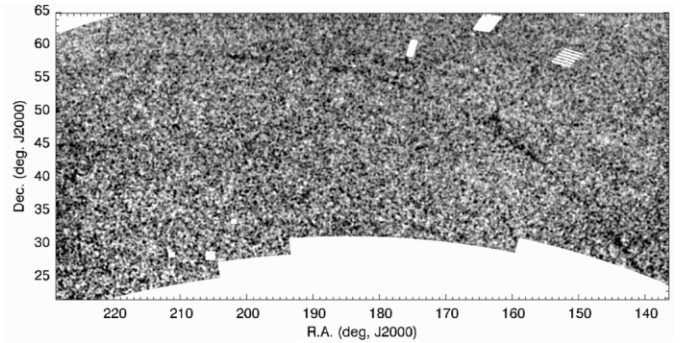


FIG. 1.—Smoothed, summed weight image of the SDSS field after subtraction of a low-order polynomial surface fit. Darker areas indicate higher surface densities. The weight image has been smoothed with a Gaussian kernel with  $\sigma = 0.2$ . The white areas are either missing data, clusters, or bright stars that have been masked out prior to analysis.

once again the rapidly increasing contamination by field stars at lower Galactic latitudes.

Sampling at several representative points, the stream appears to be  $30'$  wide (FWHM) on average. This width is similar to those observed in the tidal tails of the globular clusters Pal 5 and NGC 5466 (Grillmair & Dionatos 2006; Grillmair & Johnson 2006). On the other hand, the width is much narrower than the tidal arms of the Sagittarius dwarf (Majewski et al. 2003; Martinez-Delgado et al. 2004; one of which runs along the southern edge of the field shown in Fig. 1). This suggests that the stars making up the stream have low random velocities and that they were probably weakly stripped from a relatively small potential. Combining this with a location high above the Galactic plane (see below) suggests that the parent body is or was a globular cluster.

Integrating the background-subtracted, weighted star counts over a width of  $\approx 0.8$ , we find the total number of stars in the discernible stream to be  $1800 \pm 200$ . As is evident in Figure 1, the surface density of stars fluctuates considerably along the stream. For stars with  $g' < 22.5$ , the average surface density is  $25 \pm 5$  stars  $\text{deg}^{-2}$ , with occasional peaks of over  $70$  stars  $\text{deg}^{-2}$ .

#### 3.1. Distance to the Stream

The power of the matched filter resides primarily at the main-sequence turnoff and below, where the luminosity function increases rapidly and the stars lie blueward of the bulk of the foreground population. The blue horizontal branch can generate much higher weights per star, but the typical numbers of horizontal-branch stars in any likely progenitor are too low to account for such a continuous and well-populated stream (e.g., Grillmair & Johnson 2006). Assuming that our filter is indeed beating against the main sequence of the stream population, we can use the filter response to estimate distances. We have attempted to extract the color-magnitude distribution for the stream stars directly, but contamination by foreground stars is so high as to make differentiation between stream and field distributions highly uncertain.

Varying the shift applied to the M13 matched filter from  $-0.3$  to  $+0.7$  mag, we measured the background-subtracted, mean weighted star counts along the stream in the regions  $140^\circ < \alpha < 154^\circ$ ,  $154^\circ < \alpha < 180^\circ$ , and  $180^\circ < \alpha < 220^\circ$ . We also measured a  $1^\circ$  segment centered on the strongest concentration of stream stars at (R.A., decl.) =  $(144.1, 30.3)$ . To avoid potential problems related to a difference in age between M13 and the stream stars, we used only the portion of the filter with

$19.5 < g' < 22.5$ , where the bright cutoff is 0.8 mag below M13's main-sequence turnoff. This reduces the contrast between the stream and the background by about 40%, but still provides sufficient signal to enable a reasonably precise measurement of peak response. If our assumptions above are valid, then we are effectively measuring relative distances by main-sequence fitting.

The mean stream surface densities as a function of filter magnitude shift are shown in Figure 2. Using a distance to M13 of 7.7 kpc and fitting Gaussians to the individual profiles, we find Sun-stream distances of 7.3, 8.5, and 9.1 kpc, respectively, for the three stream segments identified above. The high-density clump at R.A. =  $144^\circ$  yields a distance of 7.7 kpc. This puts the mean distance of the stream high above the Galactic disk at  $\sim 8.5$  kpc, with the stream oriented almost perpendicularly to our line of sight. The corresponding Galactocentric distances range from 13.5 to 15 kpc. The measured distances rise more or less monotonically from southwest to northeast, as might be expected for a feature that traces a small part of an extended Galactic orbit. Based on the widths of the peaks in Figure 2, we estimate our random measurement uncertainties to be  $\approx 500$  pc.

While the match between the color-magnitude distributions of stars in M13 and those in the stream is uncertain, the relative line-of-sight distances along the stream should be fairly robust. The measurement of relative distances rests only on the assumption that the color-magnitude distribution of stream stars is uniform and that different parts of the stream will respond to filter shifts in the same way. Of course, this may not be valid if the luminosity function of stars escaping from the parent cluster changed as a function of time due to the dynamical evolution of the cluster, and a forthcoming paper will deal with possible observational support for this. Our relative distance estimates may also be subject to variations in SDSS sensitivity and completeness at faint magnitudes, although it seems reasonable to suppose that such variations will have largely averaged out on the scales with which we are dealing.

### 3.2. The Stream Progenitor

The location and the narrowness of the stream lead us to believe that the progenitor likely is or was a globular cluster. On the other hand, the stream does not pass near any of the eight globular clusters in DR4. In particular, despite the apparent similarity in color-magnitude distribution, there appears to be no way to dynamically associate the stream with M13. The distance, radial velocity, and proper-motion measurements for M13 are among the best for any globular cluster (Odenkirchen et al. 1997; Dinescu et al. 1999). Using these measurements, the projected orbital path of M13 is neither near nor aligned with the stream for either the last two or the next two orbits of the cluster. We conclude that there is almost no possibility that M13 could be the progenitor of the current stream.

Could it be that the stream might be an apogalactic concentration of tidally stripped stars from a globular cluster that is currently elsewhere in its orbit? We have integrated orbits for 39 globular clusters with measured proper motions (Odenkirchen et al. 1997; Dinescu et al. 1999; Chen et al. 2000; Dinescu et al. 2000, 2001; Siegel et al. 2001; Wang et al. 2000) to see whether their orbits are aligned with the stream at its current location. This is fraught with considerable uncertainty as even small errors in the proper motions' measurements can lead to rather large departures between the predicted and true

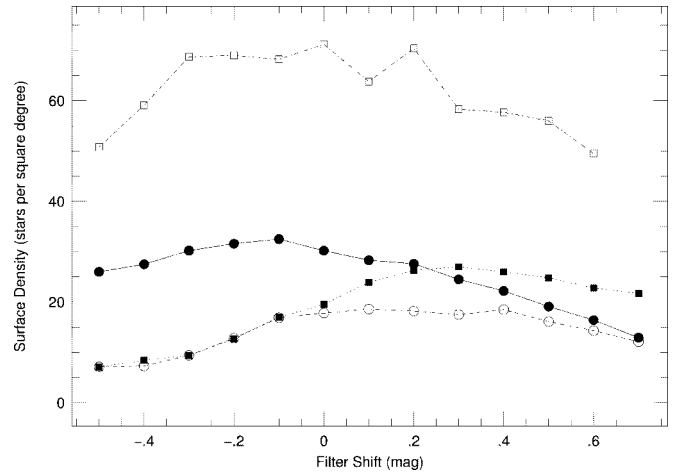


FIG. 2.—Background-subtracted, mean surface densities of stream stars as a function of the magnitude offset applied to the star count filter. Filled circles correspond to the stream segment spanning  $140^\circ < \alpha < 154^\circ$ , open circles indicate surface densities for the region  $154^\circ < \alpha < 180^\circ$ , and filled squares show the results for  $180^\circ < \alpha < 220^\circ$ . The open squares were determined for a  $1 \text{ deg}^2$  area centered on the concentration of stars at R.A., decl. =  $(144^\circ 1, +30^\circ 3)$ .

orbits of clusters. Nonetheless, as a first attempt to associate this stream with a progenitor, we integrated orbits for the 39 clusters, projected them onto the sky, and compared them with the location and orientation of the stream. We used the Galactic model of Allen & Santillan (1991), which includes a disk and bulge and assumes a spherical halo.

Only two of the 39 clusters, NGC 1904 and NGC 4590, have predicted orbits whose projections lie near the stream on the sky and are roughly aligned with it. Both of these clusters show evidence of tidal tails (Grillmair et al. 1995). However, for NGC 1904, the orbital path in the region of the stream passes within 5 kpc of the Sun. This would require a brightward shift of the M13 filter of over a magnitude, a shift that we have tested and for which the stream all but disappears. For NGC 4590, the apparent alignment with the stream is much closer, but the predicted distances at the eastern and western ends of the stream are 8.2 and 19 kpc, respectively. Thus, not only does the mean distance disagree with our estimate above, but the spatial orientation of the stream is at odds with the predicted orbit by more than  $50^\circ$ .

Where then is the progenitor of the stream? It is certainly possible that the stream represents the leavings of one of the  $\sim 108$  clusters for which we cannot yet estimate orbits. Alternatively, the source of the stream may be embedded in the stream itself. The densest portions of the stream occur at (R.A., decl.) =  $(144^\circ 13, 30^\circ 3)$  and  $(157^\circ 5, 43^\circ 7)$ , each with surface densities of over  $70 \text{ stars deg}^{-2}$ . However,  $70 \text{ stars deg}^{-2}$  to almost 4 mag below the turnoff would barely qualify as an open cluster. Examining the distribution of SDSS catalog stars directly, there appears to be no tendency for the stars to cluster in these regions. The highest density peaks in Figure 1 are probably not bound clusters and may rather be entirely analogous to similar peaks seen in the tidal stream of Pal 5, which are interpreted as a natural consequence of the episodic nature of tidal stripping. Alternatively, one of the peaks in Figure 1 could be the *remnant* of the parent cluster. The existence of such disrupted clusters would not be unexpected (Gnedin & Ostriker 1997), and Pal 5 itself is believed to have lost at least 90% of its mass and to be on its last orbit around the Galaxy (Grillmair & Smith 2001; Odenkirchen et al. 2003).

### 3.3. Constraints on the Orbit of Stream

Lacking velocity measurements, we cannot “solve” for the orbit of the stream. However, the apparent orientation of the stream, along with our estimates of its distance and curvature, can yield some constraints. Again using the Galactic model of Allen & Santillan (1991) (which Grillmair & Johnson 2006 and Grillmair & Dionatos 2006 found to work reasonably well for NGC 5466 and Pal 5), we use a least-squares method to fit both the orientation on the sky and the distance measurements in § 3.1. The tangential velocity at each point is primarily constrained by the projected path of the stream on the sky, while our distance estimates help to limit the range of possible radial velocities. We fit to a number of normal points lying along the center line of the stream and adopt a radial velocity fiducial point at the midpoint of the northeastern segment above, with R.A., decl. = (202°0, 58°4).

If we give no weight to our relative distance estimates but use only the  $9.1 \pm 0.5$  kpc estimate for the fiducial point, then for a reasonable range of radial velocities ( $-320 \text{ km s}^{-1} < v_{\text{LSR}} < 320 \text{ km s}^{-1}$ ), the perigalacticon of the stream’s orbit must lie in the range  $6.5 \text{ kpc} < R < 13.5 \text{ kpc}$ . For all LSR radial velocities in the range  $-270 \text{ km s}^{-1} < v_{\text{LSR}} < 0 \text{ km s}^{-1}$ , the apogalactic radius is constrained to fall within  $17 \text{ kpc} < R < 40 \text{ kpc}$ . On the other hand, positive radial velocities lead to orbits with apogalactica rising from 100 to 500 kpc. All of these orbits give excellent fits to the observed path of the stream on the sky.

If we constrain the model using our relative distance estimates (allowing the proper motions to become free-ranging and uninteresting parameters), we find a best-fit value for the radial velocity at the fiducial point of  $-208 \pm 30 \text{ km s}^{-1}$ , where the uncertainty corresponds to the 95% confidence interval.

The orbit corresponding to this radial velocity has  $R_p = 13.2 \pm 0.7 \text{ kpc}$  and  $R_a = 18 \pm 2 \text{ kpc}$ , where the uncertainties reflect only our estimated uncertainty in the radial velocity. For this orbit, the physical length of the visible stream would be  $\approx 9.6 \text{ kpc}$ .

## 4. CONCLUSIONS

Applying optimal contrast filtering techniques to SDSS data, we have detected a stream of stars some  $63^\circ$  long on the sky. We are unable to identify a progenitor for this stream, although from its appearance and location on the sky, we believe it to be either an extant or disrupted globular cluster. Based on a good match to the color-magnitude distribution of stars in M13, we conclude that the stars making up the stream are primarily old and metal-poor, and that the stream as a whole is about 8.5 kpc distant and roughly perpendicular to our line of sight.

Refinement of the stream’s orbit will require radial velocity measurements of individual stars along its length. Ultimately, the vetted stream stars will become prime targets for the *Space Interferometry Mission*, whose proper-motion measurements will enable very much stronger constraints to be placed on both the orbit of the progenitor and the potential field of the Galaxy.

We are grateful to Helio Rocha-Pinto for comments that significantly improved the manuscript. Funding for the creation and distribution of the SDSS Archive has been provided by the Alfred P. Sloan Foundation, the Participating Institutions, the National Aeronautics and Space Administration, the National Science Foundation, the US Department of Energy, the Japanese Monbukagakusho, and the Max Planck Society.

*Facilities:* Sloan

## REFERENCES

- Allen, C., & Santillan, A. 1991, *Rev. Mex. AA*, 22, 255  
 Belokurov, V., Evans, N. W., Irwin, M. J., Hewett, P. C., & Wilkinson, M. I. 2006, *ApJ*, 637, L29  
 Chen, L., Geffert, M., Wang, J. J., Reif, K., & Braun, J. M. 2000, *A&AS*, 145, 223  
 Combes, F., Leon, S., & Meylan, G. 1999, *A&A*, 352, 149  
 Dinescu, D. I., Girard, T. M., & van Altena, W. F. 1999, *AJ*, 117, 1792  
 Dinescu, D. I., Majewski, S. R., Girard, T. M., & Cudworth, K. M. 2000, *AJ*, 120, 1892  
 ———. 2001, *AJ*, 122, 1916  
 Gnedin, O. Y., & Ostriker, J. P. 1997, *ApJ*, 474, 223  
 Grillmair, C. J., & Dionatos, O. 2006, *ApJ*, 641, L37  
 Grillmair, C. J., Freeman, K. C., Irwin, M., & Quinn, P. J. 1995, *AJ*, 109, 2553  
 Grillmair, C. J., & Johnson, R. 2006, *ApJ*, 639, L17  
 Grillmair, C. J., & Smith, G. H. 2001, *AJ*, 122, 3231  
 Majewski, S. R., Skrutskie, M. F., Weinberg, M. D., & Ostheimer, J. C. 2003, *ApJ*, 599, 1082  
 Martinez-Delgado, D., Gomez-Flechoso, M., Aparicio, A., & Carrera, R. 2004, *ApJ*, 601, 242  
 Murali, C., & Dubinski, J. 1999, *AJ*, 118, 911  
 Odenkirchen, M., Brosche, P., Geffert, M., & Tucholke, H.-J. 1997, *NewA*, 2, 477  
 Odenkirchen, M., et al. 2001, *ApJ*, 548, L165  
 ———. 2003, *AJ*, 126, 2385  
 Rocha-Pinto, H. J., Majewski, S. R., Skrutskie, M. F., Crane, J. D., & Patterson, R. J. 2004, *ApJ*, 615, 732  
 Rockosi, C. M., et al. 2002, *AJ*, 124, 349  
 Schlegel, D. J., Finkbeiner, D. P., & Davis, M. 1998, *ApJ*, 500, 525  
 Siegel, M. H., Majewski, S. R., Cudworth, K. M., & Takamiya, M. 2001, *AJ*, 121, 935  
 Wang, J. J., Checn, L. L., Wu, Z. Y., Gupta, A. C., & Geffert, M. 2000, *A&AS*, 142, 373  
 Yanny, B., et al. 2003, *ApJ*, 588, 824